Improvements in the Measurement of Distillation Curves. 3. Application to Gasoline and Gasoline + Methanol Mixtures

Beverly L. Smith and Thomas J. Bruno*

Physical and Chemical Properties Division, National Institute of Standards and Technology, Boulder, Colorado 80305

In previous work, several significant improvements in the measurement of distillation curves for complex fluids were introduced. The modifications to the classical measurement provide for (1) temperature and volume measurements of low uncertainty, (2) temperature control based upon fluid behavior, and, most important, (3) a composition-explicit data channel in addition to the usual temperature−volume relationship. This latter modification is achieved with a new sampling approach that allows precise qualitative as well as quantitative analyses of each fraction, on the fly. Moreover, as part of the improved approach, the distillation temperature is measured in two locations. The temperature is measured in the usual location, at the bottom of the takeoff in the distillation head, but it is also measured directly in the fluid. The measurement in the fluid is a valid equilibrium thermodynamic state point that can be theoretically explained and modeled. The usual temperature measurement location (in the head) provides a temperature that is not a thermodynamic state point for a variety of reasons but which is comparable to historical measurements made for many decades. We also use a modification of the Sidney Young equation (to correct the temperatures to standard atmospheric pressure) in which explicit account is taken of the average length of the carbon chains of the fluid. In this paper, we have applied the advanced approach to samples of 91 AI gasoline and to mixtures of this gasoline with methanol (10 and 15%, vol/vol) as examples of oxygenates. On the individual fractions, we have done chemical analysis by gas chromatography (using flame ionization detection and mass spectrometry). For the methanol blends, the approach allows characterization of the azeotropic inflections in terms of fraction composition and energy content.

Introduction

One of the most important and informative properties that is measured for complex fluid mixtures is the distillation (or boiling) curve.[1] Simply stated, the distillation curve is a graphical depiction of the boiling temperature of a fluid mixture plotted against the volume fraction distilled. One most often thinks of distillation curves in the context of petrochemicals and petroleum refining, but such curves are of great value in assessing the properties of any complex fluid mixture.[2,3] For crude petroleum, the distillation curve can be divided into distinct regions that contain the following: butanes and lighter fluids, gasoline, naphtha, kerosene, gas-oil, and residue. The temperature at each of these cuts or regions provides an idea of the volatility of each cut.[4] Products resulting from petroleum crude as multicomponent mixtures, such as gasoline, diesel fuel, jet fuel, kerosene, rocket propellant, and missile fuel, are also characterized by the distillation curve as a function of volatility.

The information that can be inferred from the distillation curve extends well beyond the rough description in terms of fluid mixture volatility, however. For example, it has been possible in recent years to relate the distillation curve to operational parameters of complex liquid fuels.[5−7] These parameters include engine starting ability, vehicle drivability, fuel system icing and vapor lock, the fuel injection schedule, fuel autoignition, etc. The front end (low-temperature region) of the distillation curve of gasoline (up to ∼70 °C) is used to assess and optimize ease of starting and the potential for hot-weather vapor lock in engines. The midrange of the gasoline curve (up to a temperature of ∼100 °C) is used to assess and optimize cold-weather performance, the operational readiness of a hot engine, and the acceleration behavior of a hot engine under load.[8,9] The top range of the distillation curve is used to assess and optimize fuel economy in a hot engine. In addition to these applications to performance optimization and design, the distillation curve provides an avenue to long-term trend analysis of fuel performance, since changes in the distillation curve are related to changes in fuel performance.[6] Distillation curves are also important in evaluating the environmental impact of the use of complex liquid fuels and the reclamation of waste.

The simplest apparatus for the measurement of distillation curves as set forth in the ASTM D-86 standard embodies a device for heating the sample (either a Bunsen burner or electric heater), a liquid bath with a condensate tube, and a graduated cylinder covered with blotting paper for a calibrated volume receiver.[10] The general importance of the distillation curve has led to the availability of commercial instruments that employ microprocessor-controlled resistance heating and automated level-following (an optical method for meniscus detection) for the volume measurement and the control of distillation rate. While these instruments provide improvement in terms of convenience, there have remained serious shortcomings and opportunities for improvement.

The commercial devices determine the initial boiling temperature (IBT) with a photocell that detects the first drop to fall into the receiver.[11] This clearly produces a delayed response that usually overstates the IBT that is reported by these instruments. This delay results in a significant systematic uncertainty in the IBT; it is clearly impossible to regard this value as a state point. Moreover, it is not uncommon for complex fluids to show an initial vaporization (noted by the onset of bubbles) followed by a lull in vaporization and then the onset of sustained boiling. This subtle behavior is missed when using

* To whom correspondence should be addressed. E-mail: bruno@boulder.nist.gov. Tel.: (303) 497-5158. Fax: (303) 497-5927.

10.1021/ie060937u
Published on Web 12/08/2006

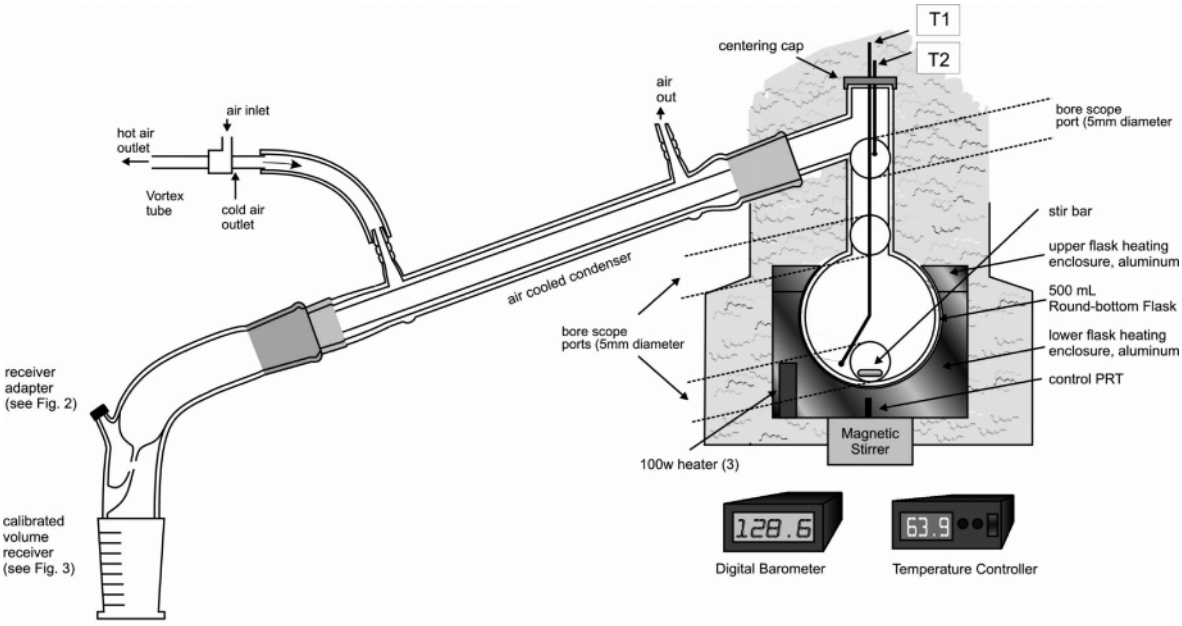

Figure 1. Schematic diagram of the overall apparatus used for the measurement of distillation curves. Note that the bore scope observation ports are only 5 mm in diameter. The size is exaggerated on the figure to make the location clear.[13]

the commercial devices. In addition, one typically selects from a menu of programmed heating profiles for a given fluid (such as a gasoline), and this preselected heating profile will influence the measured value of the IBT. Also, since the distillation flask is not stirred in the commercial devices, the potential for local superheating and nonuniformity in the horizontal direction is significant.

While the shortcomings discussed above are very serious, the information obtained from such instruments has been useful nonetheless for coarse quality control and oversight applications, especially given that most operators follow the same (or similar) procedures. The current approaches cannot be used for most design, diagnostic, or detailed applications, however. Moreover, far greater demands are placed on measurements by the desire to model fluid behavior with, for example, equations of state, and for this, the current approach is all but useless. Such equation-of-state models are required, for example, in the development of advanced technologies and in the optimization of existing technologies, where full system simulations may be desirable. In these circumstances, there is a need for measurements that are understood at a fundamental level, with much lower uncertainties, and with none of the instrument dependencies found with commercial devices. Additionally, the information content of the distillation curve can be greatly expanded by adding a composition channel to the temperature channel. By this is meant an explicit composition measurement (both qualitative and quantitative) for each boiling fraction. This is important for even complex, multicomponent fluids because the actual information that is desired from a distillation is some understanding of how the composition varies with volume fraction and boiling temperature. This is the case whether the distillation is done to design or affect a separation (fractional distillation) or as a material characterization test (simple distillation).

To address the shortcomings discussed above, improvements have been introduced that are depicted schematically in Figure 1, with additional details provided in Figures 2 and 3.[12−15] Since the major modifications have been discussed in detail elsewhere, only a relatively brief summary will be provided here. The distillation flask is a 500 mL round-bottom flask that is placed in a two-part aluminum heating jacket (alloy 6061), the lower

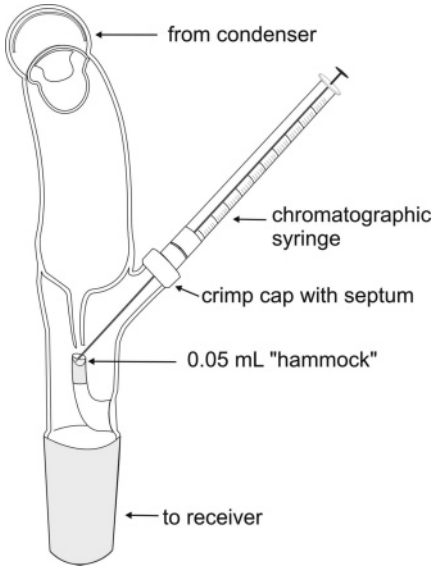

Figure 2. Schematic diagram of the receiver adapter developed for advanced distillation-curve measurements to provide on-the-fly sampling of distillate cuts for subsequent chromatographic analysis.[13]

part of which is contoured to fit the flask. The upper part is placed around the flask after the flask has been inserted into the contoured (lower) part of the jacket. This two-part enclosure effectively surrounds $\sim^4/_5$ of the spherical section of the flask. Three cartridge heaters are placed in the lower, contoured part of the jacket, arranged in a "Y" pattern, to provide uniform heating axially about the radius of the enclosure. Heating the flask in this way produces a temperature gradient in the vertical direction, while providing a very uniform temperature in the horizontal direction.

The jacket and heaters are capable of operation up to 350 °C, with a local uniformity of 0.2 °C. Note that this is the uncertainty in the control as well as in the uniformity. The jacket exterior is insulated with a Pyrex wool enclosure. This insulation extends the length of the distillation head. This ensures minimal heat leak in the vertical direction and, therefore, a small, constant temperature gradient to minimize refluxing. Three observation ports are provided in the insulation to allow penetration with a

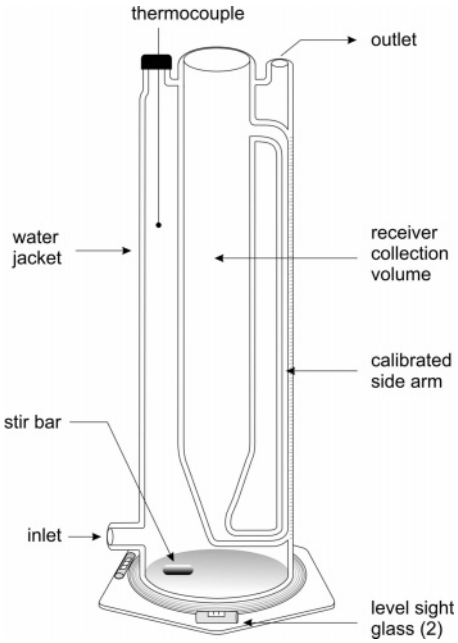

Figure 3. Schematic diagram of the level-stabilized receiver developed for advanced distillation-curve measurements.[13]

flexible, illuminated bore scope. The bore-scope ports, illustrated in Figure 1, are placed to observe the fluid in the boiling flask, the top of the boiling flask (where the spherical section joins the head, and the distillation head (at the bottom of the takeoff). Note that each of the bore-scope ports is only 5 mm in diameter; the size is exaggerated in the figure simply to make the port locations clear. The use of a bore scope for observation prevents unnecessary heat loss and subsequent loss of temperature uniformity in the horizontal direction. It also allows the operator to obtain a very close view of the fluid behavior, since the objective lens of the bore scope can be placed very close to the apparatus.

Above the distillation flask, a centering adapter provides access for two thermally tempered J-type thermocouples that enter the distillation head. One thermocouple (TC1 in Figure 1) enters the distillation flask and is submerged in the fluid, to monitor the temperature of the bulk fluid. This temperature is referred to as T_k (signifying its placement in the kettle). This thermocouple is placed well-below the surface of the fluid. The other thermocouple (TC2 in Figure 1) is centered at the low point of distillate takeoff (the typical distillation head placement, as recommended graphically in ASTM D-86). This temperature is referred to as T_h (signifying its placement in the head). Both of these thermocouples were calibrated in an indium triple-point cell traceable to a NIST standard. Monitoring both of these temperatures is critical for the advanced distillation-curve measurement. The temperature measured directly in the fluid is a true state point that can be essential for modeling studies and for comparison with theory. The temperature measured at the bottom of the distillation head takeoff point is needed to compare advanced distillation-curve measurements with measurements that have been taken for the last century.

Beneath the aluminum jacket, a magnetic stirrer drive is positioned to couple with a magnetic stir bar inside the distillation flask. Rapidly stirring the contents of the distillation flask during the measurement is essential for maintaining horizontal temperature uniformity in the fluid. Indeed, although the cartridge heaters can provide a uniformity of 0.2 °C, stirring integrates variations throughout the volume, allowing the measured temperature from T1 to be much more uniform and less uncertain. Since a vortex forms on the surface of the fluid because of the stirring, it is necessary to decrease the stirring rate as the measurement progresses, in order to prevent premature lift-out of the thermocouple, TC1, from the fluid. The lift-out of TC1 from the fluid is an inevitable result of the end of the measurement, however, and is a very useful indication of completion. This is easily recognized as a sudden upturn in temperature recorded by TC1.

The thermocouples positioned as stated above provide a rapid response to temperature. The uncertainty in the temperature measured with TC2 in the distillation head is 0.1 °C, while that of TC1 in the fluid has been found to be somewhat lower at 0.05 °C. This is partially the result of stirring, as described in the preceding paragraph.

Distillate is taken off the flask with a distillation head, into a forced-air cooled condenser. When very volatile fluids are measured, a vortex tube is used to chill the air that enters the condenser.[16−19] The vortex tube can produce a cold air stream to a temperature as low as −40 °C. Following the condenser, the distillate enters a newly designed transfer adapter that allows instantaneous sampling of distillate for chemical analysis by any applicable means. The position of the transfer adapter is shown in Figure 1 and is illustrated schematically in more detail in Figure 2.[12] The flow path of the distillate is focused to drop into a 0.05 mL "hammock" that is positioned directly below the flow path. The distillate from the condenser drops into this volume before it falls into the receiver. A crimp cap fixture is incorporated as a side arm of the adapter. This allows a replaceable crimp cap with a silicone or Teflon septum (of the type used for chromatographic automatic sampler vials) to be positioned in line with the hammock. The distance from the crimp cap to the base of the hammock is suited to the needle length of typical gas chromatographic syringes.

To sample the distillate, one simply positions the chromatographic syringe equipped with a blunt-tipped needle in the well of the hammock. It is a simple matter to withdraw samples as a function of distillate volume when a calibrated receiver is used for collection. The sample can then be directly injected into a gas chromatograph or added to a weighed vial containing an appropriate solvent for subsequent analysis off-line.

When the sample drops from the sampling transfer adapter, it flows into the calibrated receiver to allow a volume measurement. As mentioned earlier, the simple graduated cylinder that is often used for the volume measurement (and that is illustrated in ASTM D-86) is not optimal because of the relatively large uncertainty and the fact that distillate splashes into the cylinder, causing difficulty in determining the volume. The use of drop deflectors can help prevent splashing but, they can cause a higher uncertainty in the volume measurement because of holdup on the walls of the receiver. Automated optical level followers (based on photocell technology) make the volume measurement easier, but they can also be a source of uncertainty and they make it impossible to sample the distillate.[11] To improve the precision of the volume measurement, the calibrated receiver that is shown in Figure 3 was developed. Constructed of glass, this receiver consists of a central volume that gradually decreases in diameter at the base,and connects to a small-diameter side-arm sight glass that is calibrated. The side arm stabilizes the fluid level for a precise volume measurement as the distillation proceeds. The large inner volume and the sight glass are enclosed in a water jacket that contains a thermometer and a magnetic stir bar for circulation. The tube of the sight glass is actually glass-welded to the inside wall of the water jacket, to eliminate parallax in reading the volume. The water jacket

allows the receiver to be maintained at a suitable temperature, and the stirrer ensures acceptable temperature uniformity. The availability of these two sizes allows measurement of fluids with varying surface tensions. The side arm sight glass allows a volume measurement with an uncertainty of 0.05 mL. The sight glass is calibrated with the volumes of interest to the distillation curve (10−200 mL, in 10 mL increments) with a volumetric pipet.

The volume measurement in the side arm is unaffected by splashing in the collection volume, so the distillate is allowed to drop directly into the center of the collection volume space. This minimizes holdup on the walls of the vessel. Splashing causes some holdup, but this is much less than when a deflector is used. The base of the receiver is equipped with two bulls-eye type levels 90° apart to ensure that the receiver is perpendicular to the base, and liquid levels in the large volume and the side arm are collinear.

To perform a measurement, 200 mL of the fluid to be measured is placed in the round-bottom flask (typically with a 200 mL pipet), and the thermocouples are placed in the appropriate positions. This fluid volume has been chosen for convenience; any volume suitable for the measurement can be used. The temperature controller is programmed to apply a temperature profile to the distillation flask enclosure such that the enclosure temperature leads the fluid temperature by some preselected temperature, for example, 20 °C. In this way, one can achieve a constant mass flow rate through the distillation head and a measured head temperature that will be unaffected by rate aberrations that are commonly encountered in distillation-curve measurement. Starting either with a previously measured distillation curve or a calculated distillation curve (from an equation of state), an arbitrary number of "steps" can be programmed into the controller to generate the profile for the desired distillation curve.

The temperatures recorded for the distillation curve are measured at local atmospheric pressure. This must be corrected to the value that would be obtained at 1 atm. For this reason, a digital barometer is used to measure the atmospheric pressure before and after the measurement. The average of these two pressures is used to correct the temperature readings to standard atmospheric with a modification of the Sidney Young equation.[20] The procedure of ASTM-86 specifies that the correction be done with the following equation,[10]

$$C_c = C(760 - P_a)(273 + T_c) \quad (1)$$

where C_c is the correction added to the observed temperature; C is a constant, 0.000 12; P_a is the atmospheric pressure in mmHg; and T_c is the measured temperature in °C. In fact, the original Sidney Young equation specifies that C is dependent upon the average hydrocarbon chain length of the fluid, ranging from 0.000 135 for a single carbon to 0.000 119 for eight carbons. A linear correlation of these factors can be used to predict a value for simple fluids. It should be noted that the Sidney Young equation may have significant limitations when applied to correct boiling point temperatures more than 5 kPa from standard atmospheric pressure.[21] The magnitude of the correction is, of course, dependent upon the extent of departure from standard atmospheric pressure. The location of the laboratory in which the measurements reported herein is ∼1650 m above sea level, resulting in a typical temperature correction of 7 °C.

Experimental Section

The premium, winter-grade gasoline used in this work was obtained from a commercial supplier and had an antiknock index of 91. The antiknock index (AI) cited is the average of the research octane number and the motor octane number. This fluid was analyzed by gas chromatography (30 m capillary column of 5% phenyl−95% dimethyl polysiloxane having a thickness of 1 μm, temperature program from 50 to 170 °C, 7 °C/min) separately using flame ionization detection and mass spectrometric detection. This analysis showed a large fraction of aromatic constituents, consistent with the relatively high antiknock index number. Although no specific tests were done for olefin content, the GC-MS measurement mentioned above was consistent with a very low olefin content. We maintained the gasoline in a sealed container at 7 °C, to minimize moisture uptake and to ensure that no compositional changes would occur during the course of our measurements.

The dodecane used as a solvent in this work was obtained from a commercial supplier and was analyzed by gas chromatography (30 m capillary column of 5% phenyl−95% dimethyl polysiloxane having a thickness of 1 μm, temperature program from 90 to 170 °C at 7 °C per minute) using flame ionization detection and mass spectrometric detection. These analyses revealed the purity to be ∼99.9 (mass/mass) percent, and the fluid was used without further purification.

The methanol used for the gasoline oxygenate mixtures was high-performance liquid chromatography (HPLC) grade. The purity was checked with gas chromatography (30 m capillary column of 5% phenyl dimethyl polysiloxane having a thickness of 1 μm, temperature program from 50 to 100 °C at 7 °C per minute) using flame ionization detection. The purity was found to be better than 99.9%, and the fluid was used as received. The choice to measure a methanol mixture as a representative for an oxygenate gasoline requires some discussion. Although gasoline + methanol blends have been used commercially as oxygenates, the more common commercial alcohol oxygenate is, of course, made with ethanol. Despite this, methanol, which is easier to dry than ethanol, has been well-studied as an oxygenate.[22,23]

Methanol mixtures were chosen for the oxygenates in this work because this fluid causes a far more pronounced azeotropic inflection in the distillation curve than does ethanol. For this reason, the mixtures with methanol pose a much greater challenge in the measurement when a model-predictive temperature controller is employed. We, therefore, chose to focus on methanol mixtures in the development of the advanced distillation-curve approach, since the test of the temperature control of the advanced approach would be that much more stringent.[15] The methanol blends were prepared in mixing cylinders with volumetric pipettes. These mixtures were not prepared in advance but rather just before each distillation-curve measurement. The uncertainty in the volume measurement for each mixture preparation was 0.05 mL.

The measurements presented in this paper are regarded as an example of the possible information that becomes available when using the new approach to distillation-curve measurement. We realize that there are very significant composition differences between samples of commercial gasoline. Indeed, there are significant compositional differences among samples of gasoline having the same nominal octane number or antiknock index. For this reason, the results we present below are not to be construed as representative of gasoline per se; rather, they are to be considered representative of the potential of the advanced method.

The required fluid for the distillation-curve measurement (in each case, 200 mL) was placed into the boiling flask (of Figure 1) with a 200 mL volumetric pipet. The thermocouples were inserted into the proper locations, and heating commenced with a five-step program based upon a previously measured distillation curve. For these measurements, the temperature of the air in the forced-air condenser was ~8 °C. Volume measurements were made in the level-stabilized receiver, and sample aliquots were collected at the receiver adapter hammock. In the course of this work, we performed four complete distillation-curve measurements of the 91 AI gasoline and of the 10 and 15% mixtures (vol/vol) with methanol.

To provide the composition channel to accompany the temperature information on the distillation curves, sample aliquots were withdrawn for selected distillate volume fractions. These withdrawn samples were then subjected to chemical analysis. To accomplish this, aliquots of 7 μL of emergent fluid were withdrawn and added to a vial containing a known mass of solvent (*n*-dodecane). The use of *n*-dodecane as the solvent stabilized the samples in that the resulting mixture was less prone to the loss of the more volatile constituents. In this way, the *n*-dodecane serves as a solvent and as a "keeper" (in much the same way as a drop of mineral oil is used when concentrating analytical samples in a Danish Kuderna concentrator tube during a nitrogen blowdown).[24] The *n*-dodecane elutes well after all of the gasoline peaks have eluted and poses no chromatographic interference. For the gasoline samples, a gas chromatographic method was used with mass spectrometric detection. This allowed the qualitative identification of the components of each fraction, in addition to the quantitative determination. Standard mixtures of methanol in toluene and *n*-hexane were used to calibrate the response of the total ion chromatogram. Because of the complexity of the mixtures, it was not practical to calibrate for each component. The aromatic hydrocarbons were standardized with mixtures of toluene + ethyl benzene and the xylenes. The aliphatic hydrocarbons were standardized with mixtures of toluene + hexane, toluene + heptane, and toluene + 2,3-dimethyl hexane. Several mixtures of toluene + methanol were used to standardize the mixtures that contained methanol. This approach to standardization was checked with several binary mixtures (*n*-heptane + *n*-octane, *n*-octane + ethylbenzene), that were gravimetrically prepared. The uncertainty in the mole fraction determinations was ~10%, on the basis of replicate measurements. All of the measurements and checks that were performed indicate a lower uncertainty, between 6 and 8%, but we have chosen to be more conservative with 10%.

Results and Discussion

As stated above, we performed four complete distillation-curve measurements of the 91 AI gasoline and of the 10 and 15% mixtures (vol/vol) with methanol. The repeatability of the distillation curves has been discussed extensively elsewhere.[13,14] For this reason, only representative data will be presented here, along with appropriate estimates of uncertainty.

Initial Boiling Temperatures. During the initial heating of each sample in the distillation flask, the behavior of the fluid was carefully observed. Direct observation through the flask window or through the bore scope allowed measurement of the onset of boiling for each of the mixtures. Typically, the first bubbles will appear intermittently and will quell if the stirrer is stopped momentarily. Sustained vapor bubbling is then observed. In the context of the advanced distillation-curve measurement, sustained bubbling is also somewhat intermittent, but it is observable even when the stirrer is momentarily stopped. Finally, the temperature at which vapor is first observed to rise into the distillation head is observed. This is termed the vapor-rise temperature. These observations are important because they can be modeled theoretically, for example, with an equation of state.

Table 1. Summary of the Initial Behavior of the 91 AI Gasoline and the 10 and 15% Mixtures with Methanol[a]

observed temperature	91 AI gasoline, °C	91 AI gasoline + 10% MeOH (vol/vol), °C	91 AI gasoline + 15% MeOH (vol/vol), °C
onset	35.4	34.3	33.7
sustained	43.4	38.1	37.4
vapor rise	**44.4**	**42.8**	**40.4**

[a] In keeping with our advanced distillation-curve protocol, the onset temperature is the temperature at which the first bubbles are observed. The sustained bubbling temperature is that at which the bubbling persists. The vapor rise temperature is that at which vapor is observed to rise into the distillation head, considered to be the initial boiling temperature (highlighted in bold print). The uncertainties are discussed in the text.

The initial temperature observations for a representative measurement are summarized in Table 1. For example, for the 91 AI gasoline, the temperature for the appearance of the first vapor bubble was 35.4 °C, measured by TC1 in the liquid. Bubbling was observed to be sustained when the temperature of the fluid reached 43.4 °C. Vapor was observed rising into the head when the temperature reached 44.4 °C, which is considered to be the initial boiling temperature for the mixture (IBT). We make this assignment on the basis of measurements with pure fluids that were presented previously.[13,14] It is at this point that the bubbling is continuous and is observed to occur with or without stirring. These temperatures have been corrected to standard atmospheric pressure with the Sidney Young equation. The constant C in the equation was set at 0.000 119, corresponding to a typical carbon chain length of 8 units, suitable for gasoline mixtures.

Clearly, there is an element of subjectivity in determining these initial temperatures. For example, it is often difficult to distinguish between initial bubbling and the entrainment of air bubbles by the action of the stirrer. Experience with previous mixtures, including *n*-alkane standard mixtures that were prepared gravimetrically, indicates that the uncertainty in the onset and sustained bubbling temperatures is ~1 °C. The uncertainty in the vapor-rise temperature is actually much lower, at ~0.3 °C. Examination of the observed temperatures reveals a clear trend of decreasing temperature with increasing methanol concentration. This trend is consistent with expectation, since methanol makes the gasoline mixture considerably more volatile. This trend is clear when the observed temperatures are plotted against methanol concentration, in Figure 4. Here, as with Table 1, the most important observation is the vapor-rise temperature, since this is the initial boiling point of the fluid. Moreover, it is the least uncertain of these three observed temperatures.

We note in passing that these observations are very different from the initial boiling temperatures that would be obtained from a commercial ASTM D-86 instrument, in which the IBT would be recorded as the first drop of distillate enters the receiver.[11] As we have shown previously, the usual ASTM D-86 approach yields an initial boiling temperature that is between 7 and 13 °C in (systematic) error.

Distillation Curves. Representative distillation-curve data for gasoline and the oxygenate mixtures, presented in both T_k and T_h, are provided in Table 2. The reason for presenting both T_k and T_h has been discussed earlier; the T_h data allow comparison with earlier measurements. In this table, the uncertainty in the temperatures is 0.1 °C. Note that the experimental uncertainty

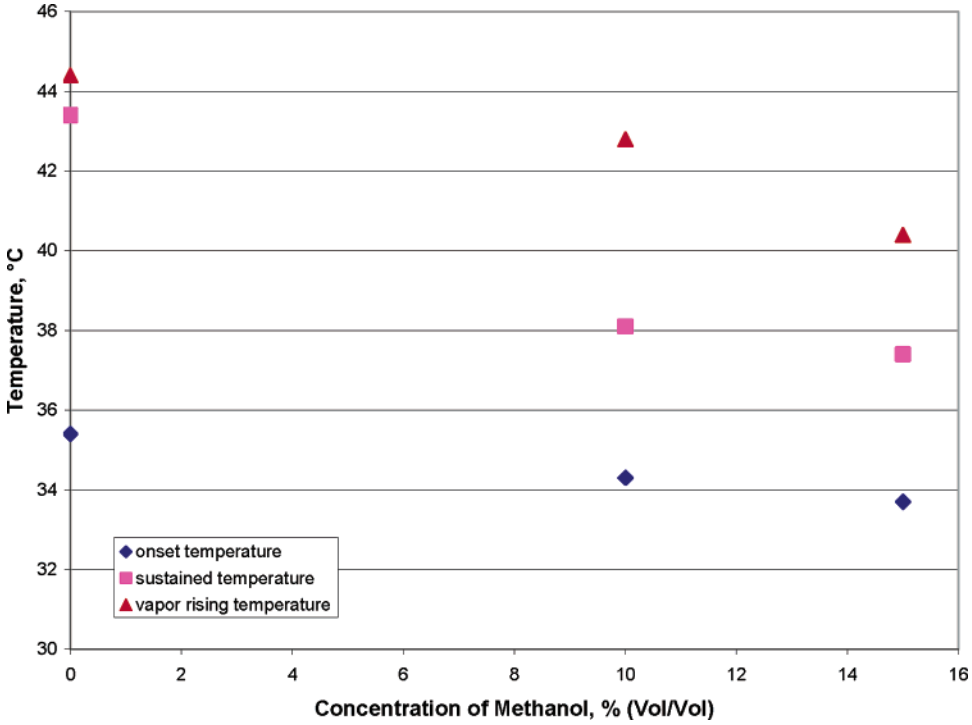

Figure 4. Plot of the initial temperature observations made during the measurement of distillation curves of the 91 AI gasoline and the 10 and 15% mixtures with methanol.

Table 2. Representative Distillation-Curve Data for 90 AI Gasoline and Mixtures of 10 and 15% (vol/vol) with Methanol

	91 AI gasoline		91 AI gasoline + 10% (vol/vol) methanol		91 AI gasoline + 15% (vol/vol) methanol	
distillate volume fraction, %	T_k, °C	T_h, °C	T_k, °C	T_h, °C	T_k, °C	T_h, °C
5	58.2	53.8	51.2	52.0	51.3	50.2
10	65.5	61.6	56.0	56.7	56.2	56.0
15	71.7	66.7	59.8	59.0	59.9	60.3
20	82.3	78.2	63.5	60.2	62.2	62.2
25	92.1	87.1	67.6	62.7	65.5	65.4
30	104.1	99.5	75.5	66.2	67.2	66.8
35	112.3	107.8	95.3	77.4	70.6	69.1
40	120.1	116.3	117.0	109.8	80.6	71.2
45	124.2	119.5	125.7	121.8	113.3	94.6
50	130.0	124.7	130.2	126.1	127.9	120.4
55	136.0	130.3	135.8	131.8	134.4	127.3
60	140.4	134.5	142.1	138.2	140.8	134.7
65	147.1	140.6	148.6	145.1	148.5	142.1
70	154.5	146.7	156.6	151.1	157.0	152.4
75	165.6	157.1	165.5	160.0	166.1	161.4
80	177.4	157.6	178.7	171.0	179.6	166.4

of T_k is somewhat lower than that of T_h, but as a conservative position, we use the higher value for both temperatures. The uncertainty in the volume measurement is 0.05 mL. The same data are provided graphically in Figure 5. The plotted curves are particularly instructive, since the expected inflections caused by the presence of methanol in the fluid are clear. We note that the presence of methanol significantly decreases the initial distillation temperature for the 10 and the 15% methanol mixtures. The inflection caused by the formation of azeotropic mixtures is then observed, followed by a gradual convergence approaching the curve for the gasoline. Both of the methanol mixtures behave similarly for the 5, 10, and 15% distillate volume fractions. Between 20 and 45%, the divergence becomes much more pronounced. From distillate volume fractions starting at 50%, continuing to 80%, all three mixtures, including the gasoline with no added methanol, essentially show the same behavior.

The relationship between the temperatures T_k and T_h can be seen in parts a and b of Figure 6, where the curves for the 91 AI gasoline and the 15% methanol mixture, respectively, are shown. It is usual for the fluid temperature, T_k, to lead the head temperature, T_h. This is especially clear when the slopes of the curves are relatively steep, as seen in both figures. When the slopes become less steep (as in the region of the azeotropic inflection caused by the presence of methanol), one can see overlap. This is a result of the mixture behaving more like a pure fluid. Indeed, we noted such behavior when the method used in this work was applied to an essentially pure fluid, the missile fuel JP-10 (exo-tetrahydrodicyclopentadiene, or tricyclo-[5.2.1.$0^{2,6}$]decane).[25] In this respect, having both temperatures T_k and T_h also serves as a diagnostic. One can be more confident that the inflections are caused by an azeotrope effect because the vapor and liquid phases of the mixture behave in a way that is similar to a pure fluid.

Composition Channel Information. (a) Hydrocarbon Type Classification. While the gross examination of the distillation curves is instructive and valuable for design, the composition channel of the advanced approach affords still greater information content. One can sample and examine the individual fractions as they emerge from the apparatus, as discussed in the introduction. Following the procedure described, samples were collected and prepared for analysis. The distillate fractions of the 91 AI gasoline and the 15% methanol (vol/vol) mixture were examined for hydrocarbon types by means of a mass spectrometric classification method summarized in ASTM Method D-2789.[26] In this method, one uses mass spectrometry, or gas chromatography−mass spectrometry, to characterize hydrocarbon samples into six types. The six types or families are paraffins, monocycloparaffins, dicycloparaffins, alkylbenzenes (or aromatics), indanes and tetralins (grouped as one classification), and naphthalenes. Although the method is

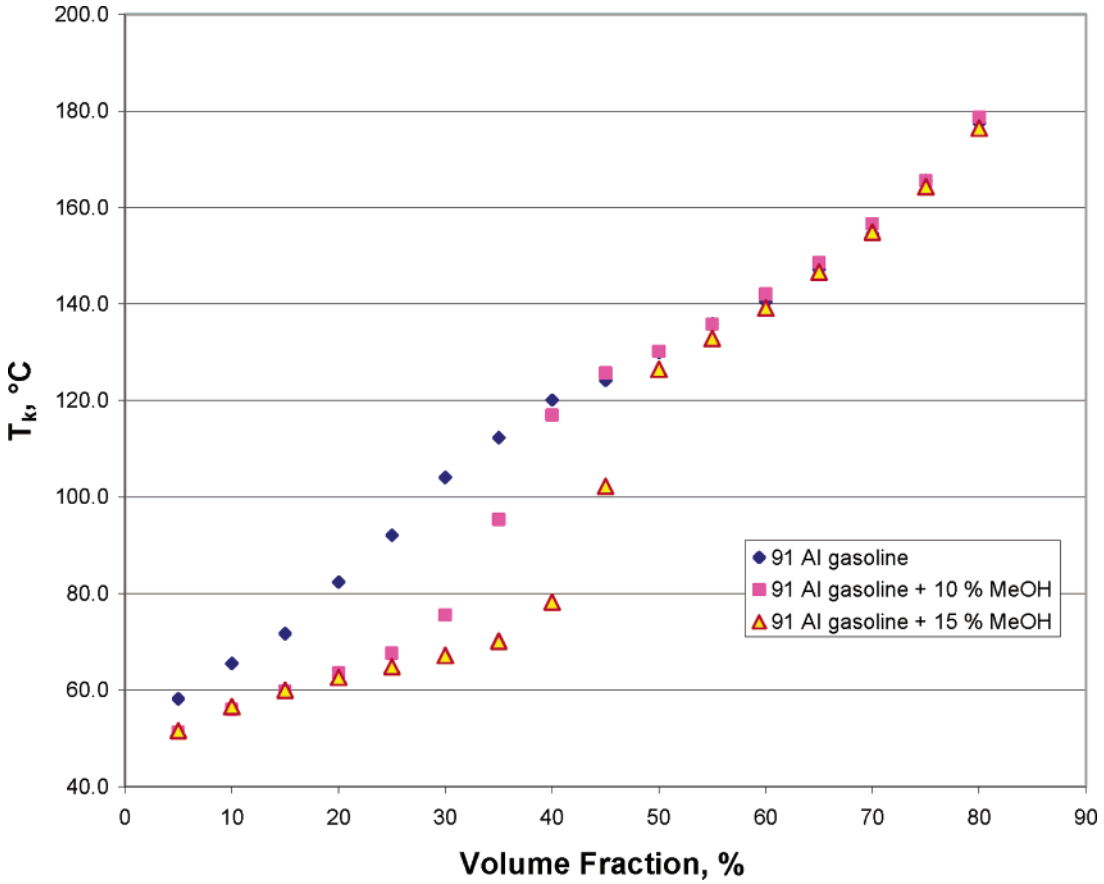

Figure 5. Distillation curves of 91 AI gasoline and 10 and 15% (vol/vol) mixtures with methanol (represented as MeOH in the figure). The temperature T_k, measured directly in the fluid, has been corrected to 1 atm with the Sidney Young equation.

specified only for application to low olefinic gasolines, it is of practical relevance to many complex fluid analyses. Indeed, it is often applied to gas turbine fuels, rocket propellants, lubricants, and many other fluids, with varying results and measures of success. The approach requires the measurement of a global mass spectrum for the sample and then the classification of the intensity values of the *m*/*z* peaks (defined as the ratio of ion mass to ion charge) for the fragments into hydrocarbon types. These family groups are then calibrated with standards and the relative percent of each type, expressed as a volume fraction, is calculated.

A comment about nomenclature is warranted, since we are using very similar terms to describe the result of the distillation-curve measurement, namely, distillate volume fraction (from the distillation-curve measurement), and the component volume fractions that result from the ASTM D-2789 calculation. The distillate volume fraction is a measured quantity that is normalized with respect to the initial fluid volume added to the distillation flask. The volume fraction that results from the ASTM D-2789 calculation is the result of a correlation and is normalized with respect to the global average mass spectrum of the entire sample. In our case, the entire sample is the aliquot withdrawn for analysis for a particular distillation volume fraction.

We have found that the reproducibility of the calculated volume fractions that result from the application of this method is ~0.3%. This was determined on the basis of replicate application of the calculation to separate average mass spectra. Note that we do not use the term uncertainty with respect to this calculation. We have found that the method can give systematically deceptive values for some of the hydrocarbon groups. When compared to volumetrically prepared standards, the volume fraction values returned for paraffins can show systematic differences of between 4 and 18%. The systematic deviations for the monocyclic and dicyclic paraffins can be even higher, especially in the presence of olefinic compounds. Thus, the method is specific for low olefinic gasolines. Despite this cautionary note, the ASTM D-2789 method can be used very effectively as an intercomparison method among related fluids and to explore trends and differences among related fluids.[27]

The hydrocarbon types that are treated by this approach are presented in Table 3, along with their fragment sums. We have omitted results for the naphthalenes, since these were not detected in the sample studied. For the 91 AI gasoline (with no added methanol), sample aliquots were collected for the distillate fractions shown in Table 4. As mentioned in the Experimental Section, the solutions were prepared from withdrawn 7 μL samples of distillate fraction in a known mass of solvent (*n*-dodecane). This solvent was chosen because it causes no interference with the sample constituents and because it stabilizes the volatile gasoline distillate fractions. For the hydrocarbon type analysis, 1 μL injections were made into the GC-MS. Because of this consistent injection volume, no corrections to the ASTM D-2789 procedure were needed for injection volume.

The hydrocarbon type breakdown resulting from the ASTM D-2789 analysis is also provided in this table. The fraction corresponding to 0.025% represents the first drop of distillate to emerge from the condenser. It is clear that, as the distillation proceeds, the fractions become rapidly more concentrated in aromatic constituents and gradually less concentrated in paraffins and monocycloparaffins. The dicycloparaffins are a very small contributor to the overall composition, and no clear trend is observable. For the indanes and tetralins, there is a gradual

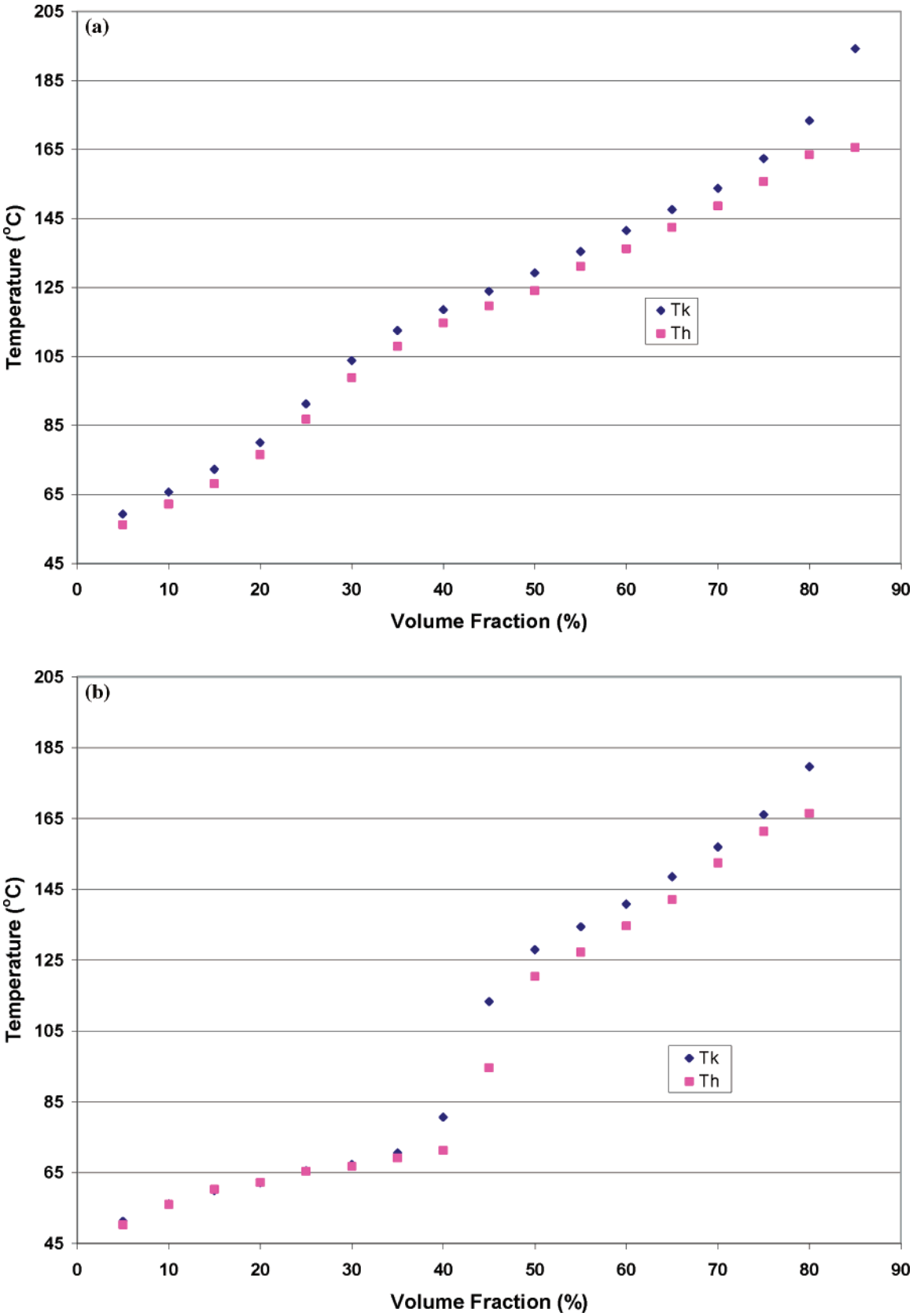

Figure 6. (a) Distillation curves of 91 AI gasoline, presented in terms of T_k and T_h. (b) Distillation curves of 91 AI gasoline + 15% methanol, presented in terms of T_k and T_h.

increase in concentration with distillate volume fraction, but this increase becomes more rapid in the later stages of the distillation. The volume fractions for the more important hydrocarbon types are plotted against emergent distillate volume fraction in Figure 7, where the trends are apparent. Similar trends within a hydrocarbon type are seen for the 15% methanol mixture as a function of distillate volume fraction.

For the 91 AI gasoline with 15% methanol, the results of the ASTM D-2789 analysis are presented in Table 5. For this mixture, we have also analyzed the residue remaining in the

Table 3. Hydrocarbon Types Delineated by ASTM D-2789 and the *m/e* Peaks Whose Intensities Are Required in the Calculation

hydrocarbontype	additiveintensityof*m/e*peaks
paraffins, Σ43	Σ43 + 57 + 71 + 85 + 99
monocycloparaffins, Σ41	Σ41 + 55 + 69 + 83 + 97
dicycloparaffins, Σ67	Σ67 + 68 + 81 + 82 + 95 + 96
alkylbenzenes, Σ77	Σ77 + 78 + 79 + 91 + 92 + 105 + 106 + 119 + 120 + 133 + 134 + 147 + 148 + 161 + 162
indanes and tetralins, Σ103	Σ103 + 104 + 117 + 118 + 131 + 132 + 145 146 + 159 + 160
naphthalenes, Σ128	Σ128 + 141 + 142 + 155 + 156

Table 4. Hydrocarbon Type from the ASTM D-2789 Analysis as a Function of Distillate Volume Fraction for the 91 AI Gasoline (with No Added Methanol)[a].

distillate volume fraction, %	paraffins	monocyclo-paraffins	dicyclo-paraffins	alkyl aromatics	indanes and tetralins
0.025	46.7	26.7	0.3	26.2	0.0
20	34.2	18.3	0.9	46.1	0.4
30	29.0	15.7	0.8	54.1	0.5
35	19.8	16.3	1.1	61.9	0.9
40	22.6	11.2	0.6	64.4	1.2
45	19.3	7.9	0.2	71.1	1.5
50	16.7	6.6	0.3	74.5	1.9
80	1.1	0.2	0.0	92.0	6.7

[a] The hydrocarbon type is presented as a normalized volume fraction, the uncertainty of which is ∼0.3%.

kettle after the distillation-curve measurement was complete. In parts a and b of Figure 8, we present a comparison between the alkyl aromatic content and the indane and tetralin content for the two mixtures. This is a different presentation from that of Figure 7; here we explore the difference between the gasoline and the oxygenate mixture. We can see that the application of the hydrocarbon type classification can provide insight into the fluid behavior. Both the alkyl aromatic content and the indane and tetralin content decrease in the area of the azeotropic inflection of the distillation curve. While we recognize that the differences revealed by the ASTM D-2789 analysis may not be entirely responsible for the differing properties, the result is instructive nonetheless. We point out that ASTM D-2789 is but one test that can be applied to distillate fraction aliquots. Indeed, any test applicable to a given situation may be applied to analyze a particular distillate fraction.

Detailed Chemical Analysis of Distillate Fractions. In addition to the very rough hydrocarbon type classification that is possible with ASTM D-2789, it is possible to perform a more detailed chemical analysis on fractions of interest. This is especially useful for diagnostic purposes. To demonstrate the potential of this aspect of the composition channel of information, we present the composition of the 0.025, 45, and 80% distillate volume fractions for the 91 AI gasoline and for the 15% (vol/vol) methanol mixture, in Tables 6 and 7, respectively. The components were identified on the basis of mass spectra of chromatographic peaks, and quantitation was done with extracted ions calibrated as described in the Experimental Section. In these tables, we have listed only the major components that are identified by gas chromatography mass spectrometry; each fraction actually contains between 50 and 125 components, most of which are omitted.

To minimize the possibility of a misidentification of a component, a strict protocol was applied to the mass spectral data. For each chromatographic peak, mass spectra were examined at the leading edge, at the trailing edge, and at the apex of each peak. This is done to ensure mass spectral purity. When two peaks closely elute, for example, there is inevitably some chemical impurity of the overlapping tails of the peak. Examining the chromatographic peak for mass spectral purity ensures that the most reliable region will be chosen for the identification. In some cases, an average over the entire peak is the most appropriate basis for examination. For each chosen mass spectrum, a background spectrum was subtracted that included traces of nitrogen and water. This simplified subsequent analysis by removing extraneous *m/z* peaks. The parent ion was identified independent of software; approximate molecular mass and isotopic calculations were done as a guide, and fragmentation patterns were noted.[28,29] A search of the NIST−EPA mass spectral database was then performed.[30] In most cases, the database search was consistent with what was expected on the basis of the initial examination of the mass spectrum.

Immediately obvious from Table 7 is the very large molar quantity of methanol that is present in the initial fraction, approaching 40% (mol/mol). By the 45% distillate volume fraction, this has dropped to ∼5% (mol/mol). Interestingly, although the detailed analyses for all of the distillate volume fractions are not shown here, by the 50% fraction, no methanol can be detected in the distillate. It is at this point that the curve again shows an inflection and rapidly approaches the gasoline curve. The presence of methanol, even at relatively low concentration, keeps the curve shape depressed, and when the methanol is completely vaporized, the remaining hydrocarbons will then rapidly vaporize.

Energy Content of Distillate Fractions. In previous work, we have demonstrated that knowledge of the enthalpy of combustion of the individual components of a distillate volume fraction provides an avenue to determine the composite enthalpy of combustion for the individual fraction.[31] Thus, we can calculate a composite enthalpy of combustion for the various fractions of the 91 AI gasoline and the methanol oxygenates. This has application in the assessment of engine performance. It is well-reported in the press and from many other sources that gasoline oxygenates have a lower energy content (and, therefore, result in lower vehicle mileage), but it is often difficult to quantify these kinds of differences. While an overall analysis and composite enthalpy calculation for the entire fuel is valuable, it is clear that coupling such information with the discrete fractions of the distillation curve is far more informative.

We present the composite enthalpy of combustion of the 0.025, 45, and 80% distillate volume fractions for the 91 AI gasoline and for the 15% (vol/vol) methanol mixture in Table 8. The combined uncertainty is also provided in parentheses. There are three contributions to the uncertainty that must be considered: the uncertainty in the pure-component enthalpy of combustion, the random uncertainty in the quantitative analytical determination, and the systematic uncertainty that can potentially be introduced by a complete misidentification of a component. The uncertainty in the pure-component enthalpy of combustion is typically provided in reliable databases as a percentage.[32] The uncertainty commonly varies between 0.2 and 3%, depending upon the original source.

The next source of uncertainty to be considered is the measured molar composition of the distillate fraction. The area counts that are obtained directly from the total ion chromatogram cannot be used for a quantitative determination. Standardization

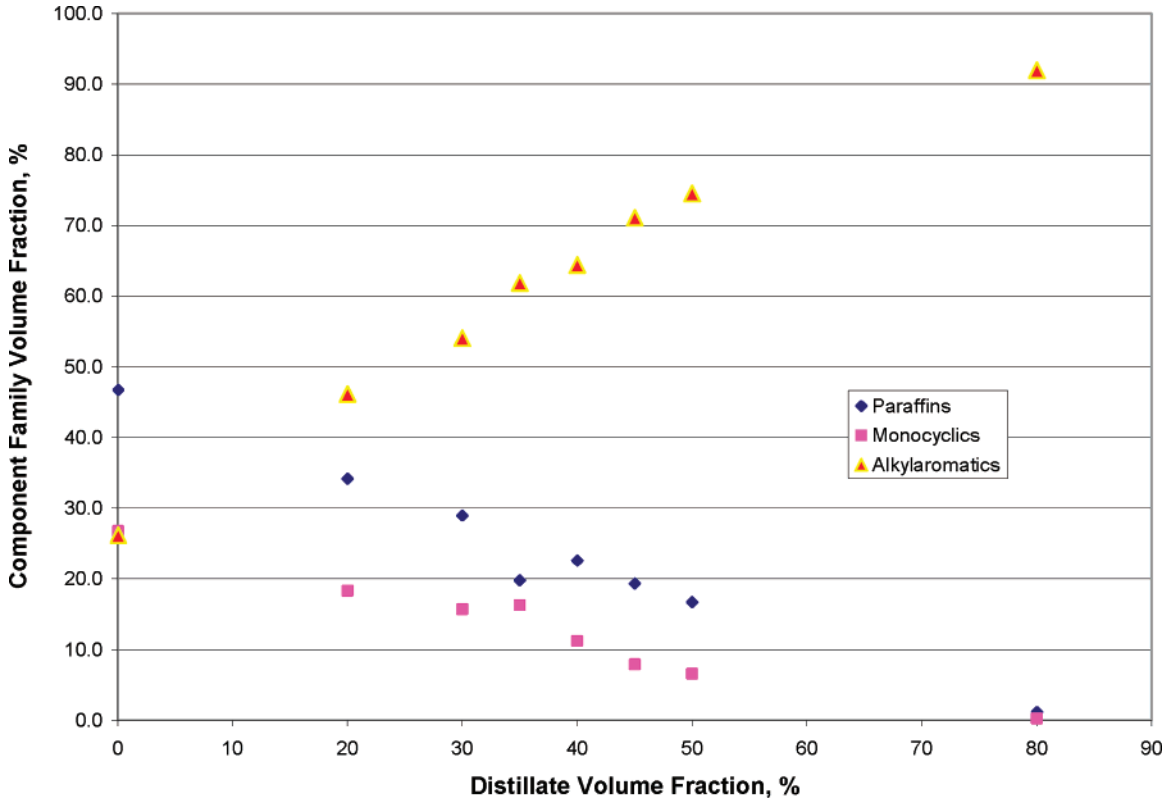

Figure 7. Plot of the volume fractions from ASTM D-2789 analysis of 91 AI gasoline as a function of emergent distillate volume fraction. Here, we have presented only the paraffins, monocycloparaffins, and alkyl aromatic hydrocarbon types.

Table 5. Hydrocarbon Type from the ASTM D-2789 Analysis as a Function of Distillate Volume Fraction for the 91 AI Gasoline + 15% (vol/vol) Methanol[a]

distillate volume fraction, %	paraffins	monocyclo-paraffins	dicyclo-paraffins	alkyl aromatics	indanes and tetralins
0.025	38.1	15.5	0.0	46.4	0.0
10	39.5	21.1	0.9	38.3	0.2
20	35.3	17.1	0.5	46.9	0.2
30	30.3	14.1	0.5	54.8	0.4
35	28.5	14.7	1.1	54.8	0.9
40	23.6	13.3	0.3	62.5	0.3
45	24.9	11.6	0.7	62.1	0.8
50	19.3	9.2	0.6	69.3	1.6
60	11.6	4.2	0.1	81.3	2.8
80	2.2	0.6	0.0	89.4	7.8
residue	0.3	0.1	0.0	91.3	8.2

[a] The hydrocarbon type is presented as a normalized volume fraction, the uncertainty of which is ~0.3%.

is required, and this is done on the basis of extracted ions (sometimes called single ion monitoring, SIM).[29] Several mixtures of toluene + methanol were used to standardize the mixtures that contained methanol. The methanol mole fractions are, therefore, known to within 1%. The aromatic hydrocarbons were standardized with mixtures of toluene + ethyl benzene and the xylenes. The aliphatic hydrocarbons were standardized with mixtures of toluene + hexane, toluene + heptane, and toluene + 2,3-dimethyl hexane. The standardization was checked with binary mixtures containing other aliphatic hydrocarbons. Since we were unable to standardize for each component (because of the multiplicity of components found in gasoline), we assign an uncertainty in our measured composition of each component in the individual gasoline fractions to be 10%.

The next source of uncertainty that we will consider is the possibility of a complete misidentification of the component. This would, of course, lead to the application of the incorrect pure-component enthalpy of combustion. Difficulties sometimes arise in differentiating closely related isomers of species that are found in relatively low concentrations (that is, with small peaks). In some cases, only the parent ion and one fragment ion *m*/*e* peak were available for up to three components (or chromatographic peaks). These could only be identified as an isomeric family (for example, the *x*,*y*-diethyl benzenes in Table 6). In these cases, the order of the isomers was determined by published retention indices or by past experience with the stationary-phase characteristics. The difference in the enthalpy of combustion between these kinds of closely related isomers is very small, typically far less than the experimental uncertainty in the measurement. As a conservative position, however, we adjusted the contribution to the overall uncertainty when, in these cases, the identity of the component was somewhat uncertain. Here, we used a coverage factor of 2.5 instead of 2 in the uncertainty propagation of the mole fraction to obtain the uncertainty of the composite enthalpy of combustion. The combined effects of these three major sources of uncertainty were considered in determining the overall uncertainty of the composite enthalpy of combustion for the gasoline fractions. This resulted in an overall 4.1% uncertainty.

There is a dramatic difference in the energy content of the two fluids in the early part of the distillation curve. For the 0.025 distillate volume fraction, this difference is ~33%. Recall that this part of the distillation curve of gasoline motor fuels is indicative of ease of starting and the potential for hot-weather vapor lock in engines. At the midrange of the distillation curve, the difference is still very large at 14%. This region of the curve is indicative of cold-weather performance, the operational readiness of a hot engine, and the acceleration behavior of a hot engine under load. We note that, at the latter part of the curve, the composite enthalpies of combustion of the two

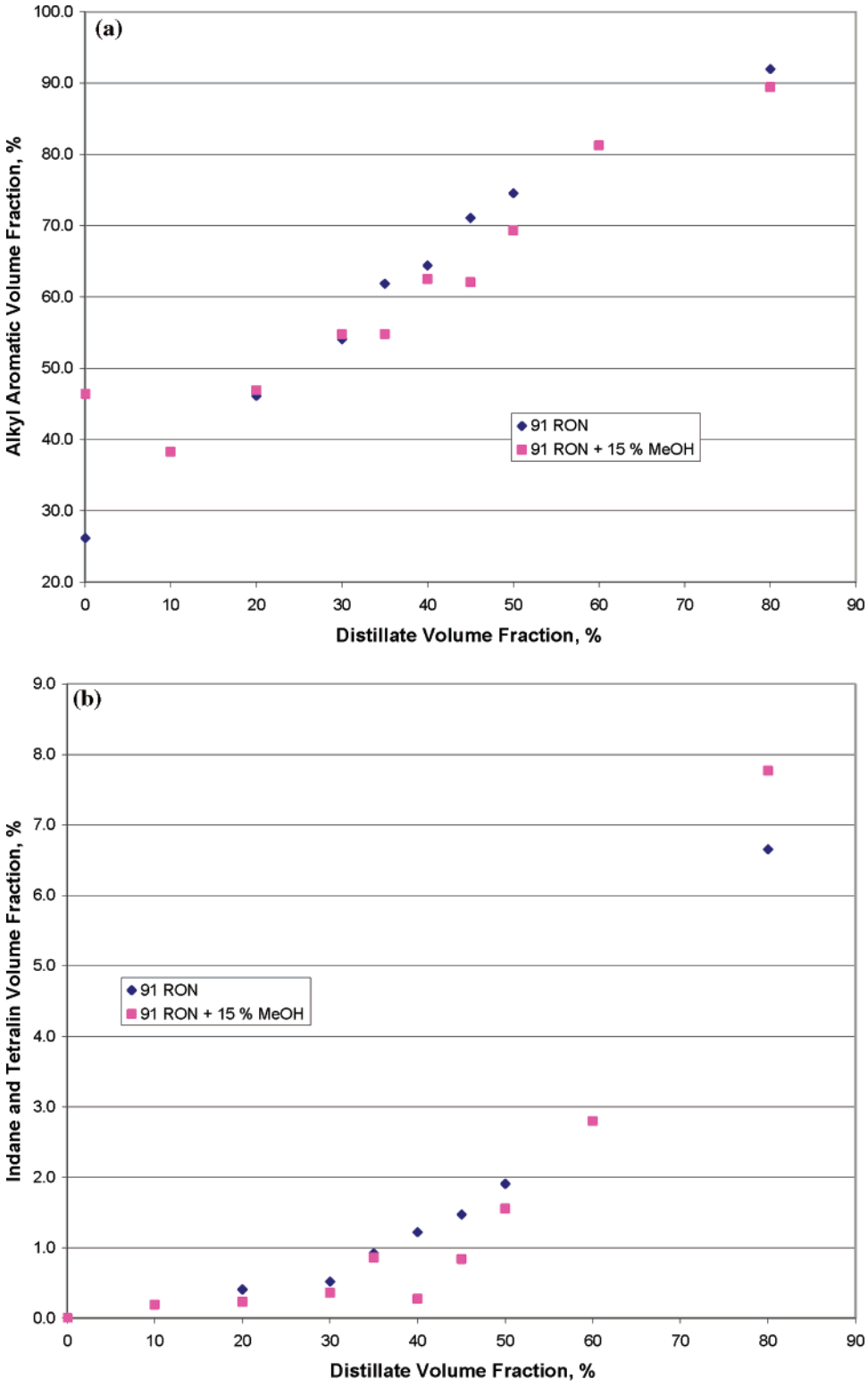

Figure 8. (a) Comparison of the alkyl aromatic content of 91 AI gasoline and the same gasoline with 15% methanol, as determined by ASTM D-2789. For the methanol mixture, in the region of the azeotropic inflection, the alkyl aromatic content is observed to decrease somewhat as a function of distillate volume fraction, relative to the pure gasoline. (b) Comparison of the indane and tetralin content of 91 AI gasoline and the same gasoline with 15% methanol, as determined by ASTM D-2789. For the methanol mixture, in the region of the azeotropic inflection, the indane and tetralin content is observed to decrease somewhat as a function of distillate volume fraction, relative to the pure gasoline.

mixtures begin to approach one another. Indeed, by the 80% distillate volume fraction, they are the same, within experimental uncertainty.

The presentation of the thermochemical information in units of kJ/mol is especially useful for design and modeling studies, since thermochemical information presented in this way represents fundamental values. A practical alternative would be a presentation in terms of volume, expressed as kJ/L. This is a simple change, requiring only the density of each identified compound at a particular temperature of interest. Thus, for the data in Table 8, one can find the liquid molar volumes (or densities) of each constituent at 25 °C and calculate the composite enthalpy of combustion for the 91 AI gasoline as 30 751 kJ/L and that of the 91 AI gasoline + 15% methanol as

Table 6. Listing of the Compounds Determined for the Distillation Curve of 91 AI Gasoline

compound	% composition (mol/mol)	compound	% composition (mol/mol)
		0.025% distillate volume fraction	
2-methyl butane	23.4	*n*-heptane	2.4
2-methyl pentane	17.6	2,3,3-trimethyl butene	0.7
n-hexane	7.7	toluene	18.6
benzene	5.1	ethyl benzene	1.0
methyl cyclopentane	16.1	1,4-dimethyl benzene	3.8
2,2,3,3-tetramethyl butane	3.8	1,2-dimethyl benzene	0.9
		45% distillate volume fraction	
2-methyl pentane	1.0	toluene	31.7
3-methyl pentane	0.7	*n*-octane	0.8
n-hexane	1.4	ethyl benzene	4.5
2,2-dimethyl pentane	1.6	1,4-dimethyl benzene	15.6
benzene	9.3	1,2-dimethyl benzene	4.8
2,2,3,3-tetramethyl butane	4.0	propyl benzene	0.7
n-heptane	3.6	1-ethyl-2-methyl benzene	3.0
2,3-dimethyl hexane	1.7	1,3,5-trimethyl benzene	0.8
2,3,4-trimethyl pentane	9.4	1,2,3-trimethyl benzene	0.5
3-ethyl-2-methyl pentane	1.2	1,2,4-trimethyl benzene	2.5
2-methyl heptane	1.5		
		80% distillate volume fraction	
toluene	1.1	indane	1.6
ethyl benzene	2.9	1-methyl-4-propyl benzene	3.1
1,4-dimethyl benzene	12.9	1-ethyl-2,4-dimethyl benzene	4.0
1,2-dimethyl benzene	6.5	1-ethyl-3,5-dimethyl benzene	9.9
1,2,3-trimethyl benzene	1.7	2-ethyl−1,3- dimethyl benzene	1.3
propyl benzene	2.7	1-methyl-3-(1-methylethyl) benzene	1.3
1-ethyl-2-methyl benzene	15.1	2-ethyl-1,4-dimethyl benzene	2.4
1,2,4-trimethyl benzene	6.5	*x*,*y*-diethyl benzene	0.3
1-ethyl-4-methyl benzene	3.4	*x*,*y*-diethyl benzene	1.1
1,3,5-trimethyl benzene	20.7	*x*,*y*-diethyl benzene	1.5

Table 7. Listing of the Compounds Determined for the Distillation Curve of 91 AI Gasoline + 15% Methanol

compound	% composition (mol/mol)	compound	% composition (mol/mol)
		0.025% distillate volume fraction	
methanol	39.5	benzene	7.1
2-methyl butane	6.1	3-methyl hexane	1.9
n-pentane	4.7	2,2,4-trimethyl pentane	2.4
2-methyl pentane	5.9	toluene	18.7
3-methyl pentane	2.7	*p*-xylene	4.6
n-hexane	3.7	ethylbenzene	1.3
methyl cyclopentane	1.4	benzene	7.1
		45% distillate volume fraction	
methanol	5.4	2,3,3-trimethyl pentane	0.8
2-methyl pentane	2.3	2-methyl heptane	1.4
3-methyl pentane	1.6	toluene	32.8
n-hexane	3.0	2,4-dimethyl heptane	0.6
2,4-dimethyl pentane	1.5	ethyl benzene	3.5
methyl cyclopentane	1.5	1,3-dimethyl benzene	11.4
benzene	11.4	1,4-dimethyl benzene	3.3
3-methyl hexane	4.0	1-ethyl−2-methyl benzene	0.4
2,2,3,3-tetramethyl butane	5.3	1-methyl ethyl benzene	1.7
n-heptane	2.9	1-ethyl-3-methyl benzene	0.4
methyl cyclohexane	1.2	1-ethyl-4-methyl benzene	0.3
2,4-dimethyl hexane	0.8	1,2,3-trimethyl benzene	1.4
2,3,4-trimethyl pentane	1.1	2,3,3-trimethyl pentane	0.8
		80% distillate volume fraction	
toluene	1.3	1,2,3-trimethyl benzene	5.7
ethylbenzene	3.4	indane	2.2
1,3-dimethyl benzene	14.2	1,3-diethyl benzene	1.0
1,2-dimethyl benzene	7.3	1-methyl-3-propyl benzene	3.8
1-methylethyl benzene	0.5	1-methyl-2-propyl benzene	2.8
propyl benzene	3.4	2-ethyl-1,4-dimethyl benzene	3.7
1-ethyl-3-methyl benzene	0.6	1-methyl-2-propyl benzene	1.0
1,2,4-trimethyl benzene	6.8	1-methyl-2-(methylethyl) benzene	4.3
1-ethyl-2-methyl benzene	4.4	1-ethyl-2,4-dimethyl benzene	4.3
1,3,5-trimethyl benzene	23.1	1,2,3,5-tetramethyl benzene	0.6
2-methylpropyl benzene	0.3	1,2,3,4-tetramethyl benzene	1.8
1-methyl-4-propyl benzene	0.3	1,2,4,5-tetramethyl benzene	2.9

25 680 kJ/L. On a volume basis, the difference is 16.5% at 25 °C. While enthalpies of combustion presented in kJ/mol have very little temperature dependence, those presented in kJ/L may be expected to have a significant temperature dependence. Still another practical alternative would be to present the thermochemical parameters on a mass basis. While the database can provide a variety of mass-based units, it is a simple matter to convert the molar-based units to J/g. On this basis, again for

Table 8. Composite Enthalpies of Combustion as a Function of Distillate Fraction for the Two Gasoline Mixtures[a]

distillate volume fraction, %	$-\Delta H_c$, composite, kJ/mol, gasoline	$-\Delta H_c$, composite, kJ/mol, gasoline + 15% methanol	percent difference
0.025	3708.5 (152)	2510.2 (93)	33.1
45	4523.1 (185)	3869.7 (158)	14.4
80	4937.8 (202)	4929.9 (202)	0.2

[a] The uncertainties (also in kJ/mol) for each composite enthalpy are provided in parentheses. The percent difference between the two gasoline mixtures is included as well.

the fractions presented in Table 8, the composite enthalpy of combustion for the 91 AI gasoline will be 43 815 J/g and that of the 91 AI gasoline + 15% methanol will be 33 574 J/g. The difference on a mass basis is, therefore, ~23%.

Conclusions

In this paper, we have reported the application of an advanced method of distillation-curve measurement as applied to gasoline and gasoline oxygenate mixtures. The measurement of the temperatures T_k and T_h provides a lower overall uncertainty and allows comments to be made about the fluid behavior. The composition channel of information provides access to more detailed insight into the fluid behavior. For example, the concentration of methanol can be followed as it decreases through the early stages of the distillation curve of the oxygenates, to the point of its disappearance. Finally, we have shown how the composition channel allows the combination of thermochemical data with the temperature data of the distillation curve. This provides an explicit measure of the energy content of each fraction.

Acknowledgment

One of us (B.L.S.) acknowledges a Professional Research Experiences Program (PREP) undergraduate fellowship at NIST. While not directly a source of funding for this work, we acknowledge that this work was an outgrowth of work done for the Air Force Research Laboratory, MIPR F4FBEY5102G001.

Literature Cited

(1) Leffler, W. L. *Petroleum Refining in Nontechnical Language*; PennWell: Tulsa, OK, 2000.

(2) Kister, H. Z. *Distillation Design*; McGraw-Hill: New York, 1991.

(3) Kister, H. Z. *Distillation Operation*; McGraw-Hill: New York, 1988.

(4) Manovyan, A. K.; Khachaturova, D. A.; Lozin, V. V. Method for determination of distillation curve of heavy petroleum products. *Chem. Technol. Fuels Oils* **1983**, *19*, 259−261.

(5) Orbital Engine Company. *Market barriers to the uptake of biofuels study: A testing based assessment to determine the impacts of a 20% ethanol gasoline fuel blend on the Australian passenger fleet*; Report to Environment Australia, 2003.

(6) Orbital Engine Company. *A literature review based assessment on the impacts of a 20% ethanol gasoline fuel blend on the Australian vehicle fleet*; Report to Environment Australia, 2002.

(7) Visser, B. Autogas vs. avgas: The differences can be major if not properly managed. *Gen. Aviat. News* **2004**, 1.

(8) Hallett, W. L. H.; Ricard, M. A. Calculations of the auto-ignition of liquid hydrocarbon mixtures as single droplets. *Fuel* **1991**, *71*, 225−229.

(9) Emel'yanov, V. E.; Grebenshchikov, V. P.; Golosova, V. F.; Baranova, G. N. Influence of gasoline distillation curve on carburetor icing. *Khim. Tekh. Top. i Masel* **1982**, *11*, 22−23.

(10) *Standard Test Method for Distillation of Petroleum Products at Atmospheric Pressure*; ASTM Standard D 86-04b, Book of Standards Vol. 05.01; American Society for Testing and Materials: West Conshohocken, PA, 2004.

(11) Babinsky, N. Koehler Instrument Company, Inc.: Bohemia, NY; Personal communication, 2005.

(12) Bruno, T. J. Method and apparatus for precision in-line sampling of distillate. *Sep. Sci. Technol.* **2006**, *41*, 309−314.

(13) Bruno, T. J. Improvements in the measurement of distillation curves. 1. A composition-explicit approach. *Ind. Eng. Chem. Res.* **2006**, *45*, 4371−4380.

(14) Bruno, T. J.; Smith, B. L. Improvements in the measurement of distillation curves. 2. Application to aerospace/aviation fuels RP-1 and S-8. *Ind. Eng. Chem. Res.* **2006**, *45*, 4381−4388.

(15) Smith, B. L.; Bruno, T. J. Advanced distillation curve measurement with a model predictive temperature controller. *Int. J. Thermophys.* **2006**, *27*, 1419−1434.

(16) Bruno, T. J. Vortex cooling for subambient temperature gas chromatography. *Anal. Chem.* **1986**, *58*, 1595−1596.

(17) Bruno, T. J. Laboratory applications of the vortex tube. *J. Chem. Educ.* **1987**, *64*, 987−988.

(18) Bruno, T. J. Applications of the vortex tube in chemical analysis. *Process Control Qual.* **1992**, *3*, 195−207.

(19) Bruno, T. J. A simple and efficient low-temperature sample cell for infrared spectrophotometry. *Rev. Sci. Instrum.* **1992**, *63*, 4459−4460.

(20) Young, S. Correction of boiling points of liquids from observed to normal pressures. *Proc. Chem. Soc.* **1902**, *81*, 777.

(21) Karonis, D.; Lois, E.; Stournas, S.; Zannikos, F. Correlations of exhaust emissions from a diesel engine with diesel fuel properties. *Energy Fuels* **1998**, *12*, 230−238.

(22) Furey, R. L. Volatility characteristics of gasoline -alcohol and gasoline-ether fuel blends. In *SAE Technical Paper Series*, Proceedings of International Fuels and Lubricants Meeting and Exposition, Tulsa, OK, Oct 21, 1985; Society of Automotive Engineers: Warrendale, PA, 1985; Paper 852116.

(23) Furey, R. L.; Perry, K. L. Vapor pressures of mixtures of gasolines and gasoline-alcohol blends. In *SAE Technical Paper Series*, Proceedings of International Fuels and Lubricants Meeting and Exposition, Philadelphia, PA, Oct 6, 1986; Society of Automotive Engineers: Warrendale, PA, 1986; Paper 861557.

(24) Bruno, T. J. Simple, inexpensive apparatus for sample concentration. *J. Chem. Educ.* **1992**, *69*, 837−838.

(25) Bruno, T. J.; Huber, M. L.; Laesecke, A.; Lemmon, E. W.; Perkins, R. A. *Thermochemical and thermophysical properties of JP-10*; NIST-IR 6640; National Institute of Standards and Technology: Gaithersburg, MD, 2006.

(26) *Standard test method for hydrocarbon types in low olefinic gasoline by mass spectrometry*; ASTM Standard D 2789-04b, Book of Standards Vol. 05.01; American Society for Testing and Materials: West Conshohocken, PA, 2005.

(27) Magee, J. W.; Bruno, T. J.; Friend, D. G.; Huber, M. L.; Laesecke, A.; Lemmon, E. W.; McLinden, M. O.; Perkins, R. A.; Baranski, J.; Widegren, J. A. *Thermophysical Properties Measurements and Models for Rocket Propellant RP-1: Phase I*; NIST-IR 6644; National Institute of Standards and Technology: Gaithersburg, MD, 2006.

(28) Bruno, T. J.; Svoronos, P. D. N. *CRC Handbook of Fundamental Spectroscopic Correlation Charts*; Taylor and Francis CRC Press: Boca Raton, FL, 2005.

(29) Bruno, T. J.; Svoronos, P. D. N. *CRC Handbook of Basic Tables for Chemical Analysis*, 2nd ed.; CRC Press: Boca Raton, FL, 2004.

(30) NIST/EPA/NIH Mass Spectral Database, S. R. D. SRD Program, National Institute of Standards and Technology: Gaithersburg, MD, 2005.

(31) Bruno, T. J.; Smith, B. L. Enthalpy of combustion of fuels as a function of distillate cut: Application of an advanced distillation curve method. *Energy Fuels* **2006**, *20*, 2109−2116.

(32) Rowley, R. L.; Wilding, W. V.; Oscarson, J. L.; Zundel, N. A.; Marshall, T. L.; Daubert, T. E.; Danner, R. P. *DIPPR(R) Data Compilation of Pure Compound Properties*; Design Institute for Physical Properties, A.: New York, 2004.

Received for review July 19, 2006
Revised manuscript received October 18, 2006
Accepted October 24, 2006

IE060937U